J Mater Sci (2010) 45:3270–3275
DOI 10.1007/s10853-010-4338-2

Electronic and optical properties of monoclinic and rutile vanadium dioxide

Guang-Hua Liu · Xiao-Yan Deng · Rui Wen

Received: 7 December 2009 / Accepted: 18 February 2010 / Published online: 6 March 2010

Abstract The electronic and optical properties of vanadium dioxide are investigated in the frameworks of density functional theory and GGA+U, in detail. It is found that, the metal–insulator transition in VO_2 is induced by the on-site correlation effects, accompanied with a distinct charge-transfer. Unlike that in rutile phase, the energy gap in the monoclinic phase opens suddenly and abruptly, which is consistent with the experimental observation. The calculated indirect energy gap (0.32 eV) and the direct energy gap (0.58 eV) can be used to theoretically interpret the experimental optical transmission at 0.31 eV and the optical energy gap 0.6 eV, respectively. Consequently, both of them are confirmed by our optical calculation. Furthermore, our calculated optical absorption peaks agree with the experiment very well.

Introduction

The observation of a metal–insulator transition (MIT) at the transition temperature 340 K in vanadium dioxide [1] has initiated many experimental [2–9] and theoretical [10–14] investigations for several decades. At high temperature, VO_2 is metallic and forms tetragonal rutile (R) structure with space group $P4_2/mnm$. While, at low temperature, it forms monoclinic (M1) structure with space group $P2_1/c$, and becomes insulator with a band gap of 0.6 eV [15]. The striking feature of M1 phase is the monoclinic distortion of R phase involving a zigzag-type dimerization (pairing) of vanadium ions along the rutile c-axis. The MIT occurs with an accompanying structural phase transition (SPT) between the monoclinic and the rutile tetragonal structures. It is commonly accepted that Peierls and Mott–Hubbard pictures are two main alternative mechanisms for MIT in VO_2. It is well known that, a Mott insulator undergoes a first-order MIT via the breakdown of a strongly correlated critical electron Coulomb interaction without a SPT [16, 17]. However, a Peierls insulator is caused by electron–phonon interaction such as a charge–density wave [18]. The Peierls MIT is then accompanied by a SPT, in another words, the MIT and the SPT occur simultaneously without the first-order MIT [6]. Up to date, there is still a debate on the MIT mechanism [11, 12]. All the controversial arguments are all based on a preconception that the MIT and the SPT occur simultaneously. However, some experiments have found that the MIT can take place independent of SPT [4–6, 19, 20], recently.

Simultaneously, the electrical and optical properties of VO_2 have also been studied extensively [21–24]. The electronic contribution to the optical properties of VO_2 had been studied by Verleur et al. [23], experimentally. Furthermore, the optical constants of M1 and R phase VO_2 (between 0.25 and 5 eV) had been determined. In M1 structure, they had found several absorption peaks centered near photon energy 0.85, 1.3, 2.8, and 3.6 eV, and the energy gap had been estimated to be about 0.6 eV. Additionally, an abrupt change from transparency to a low-limiting transmission of 0.09 near phase transition point had been observed at photon energy 0.31 eV, well above

G.-H. Liu (✉)
Department of Physics, Tianjin Polytechnic University,
300160 Tianjin, China
e-mail: ghliu@pku.edu.cn

G.-H. Liu · R. Wen
School of Physics, Peking University, 100871 Beijing, China

X.-Y. Deng
Graduate Department, Tianjin Polytechnic University, 300160
Tianjin, China

the fundamental phonon region but below the strong interband transition. However, the authors had contributed such interesting optical transmission to the free-carrier-dominated behavior. Subsequently, the reflectivity of a thick sputtered film of VO_2 had been measured in the energy range 0.5–11.0 eV at room temperature [25]. In spite of the lack of a theoretical band-structure calculation, the singularities in imaginary (ε_2) parts of the dielectric constant at 0.6, 1.04, 1.32, 1.82, 2.64, 3.6, 5.89, and 9.6 eV are assigned to specific interband transitions. In most cases, the stoichiometry, chemical purity, and freedom from defects of the measured VO_2 have been high, and this fact has produced a very large dispersion in the published data.

Regretfully, the theoretical interpretation of the experimental optical observations, especially first principle calculation, is still deficient up to date. So, in this letter, we would like to try to provide a theoretical interpretation by calculating the electronic and optical properties of the vanadium dioxide, including the band structure, the atomic or bonding population, and the optical constants. Our investigations may be helpful for us to comprehend the optical observation and search for the MIT mechanism in vanadium dioxide, theoretically. All of our calculations are performed based on the density functional theory (DFT), and the strongly correlated effects are taken into account.

Computational method

Density functional theory has become an increasingly popular tool for computational material science (seen in a recent review article [26]). Despite the widespread popularity and success of DFT, it is found to suffer from some inherent defects and limitations. Many works [27–32] have been done to try to improve them, recently. The numerical results from the local density approach (LDA) cannot describe the MIT in VO_2 satisfactorily. It is suggested that this failure is mainly due to the neglect of the local Coulomb interaction, which may be significant in 3d transitional metal oxides. So, we performed a comprehensive study of such system, in which the on-site Coulomb repulsion effects are in consideration. CASTEP code [33] is employed to calculate the total energy and the electronic properties by first principle calculations based on a plane wave basis set with periodic boundary condition. The electron–electron exchange and correlation effects are described by revised Perdew–Burke–Eruzerhof (RPBE) functional [34] in generalized gradient approximations (GGA)[35] within the DFT. Ultrasoft pseudo-potentials [36], known for their high efficiency in calculating the structural and electronic properties, are used for the electron–ion interactions. In this case, a $5 \times 6 \times 6$ Monkhorst–Pack grid and a total number of 45 k points in the irreducible Brillouin zone were employed. In order to confirm the convergence of the calculation, the cutoff energy is 340 eV, which corresponds to a criterion of convergence of 0.1×10^{-5} eV/atom. For a large class of compounds, so-called correlated systems, a mixture of the Hubbard model theory and DFT are required. The most popular implementation is known as the LDA+U method as introduced by Anisimov et al. [37]. The LDA+U method, adopting a simplified, rotationally invariant approach [38, 39] as an implementation for GGA, is applied in our calculations. For simplicity, hereafter, we call it GGA+U method. The only external parameter needed for GGA+U is the effective value of the on-site Coulomb parameter, U_{eff}, for each affected orbital. In the GGA+U method, the effective parameter $U_{\mathrm{eff}} = U - J$ is adopted as an only input parameter, where U and J are the Coulomb and exchange parameters, respectively. In order to detect the correlation effects, the effective parameter U_{eff} for V are ranging from 0 to 5.0 eV.

Population analysis in CASTEP is performed using the Mulliken formalism [40]. It is widely accepted that the absolute magnitude of the atomic charges yielded by population analysis have little physical meaning, since they display a high degree of sensitivity to the atomic basis set with which they were calculated [41]. However, consideration of their relative values can yield useful information [42], provided a consistent basis set is used for their calculation. In addition to providing an objective criterion for bonding between atoms, the overlap population may be used to assess the covalent or ionic nature of a bond. A high value of the bond population indicates a covalent bond, while a low value indicates an ionic interaction. See Segall et al. [42] for more details.

Two different initial crystalline structures of VO_2, namely high-temperature R phase with space group $P4_2/mnm$ and low-temperature M1 phase with space group $P2_1/c$ are considered (as shown in Fig. 1). The structural parameters for these two phase used in our work are taken from McWhan et al. [43] and Longo et al. [44], which are under the temperatures of $\sim$360 and 300 K, respectively.

Results and analysis

First, we calculate the overlap population (bond population) between the center V atom and its six O ligands. The results show that the V–O bond populations are dependent on the distance between them sensitively, but independent of the on-site Coulomb interaction U_{eff}. The average overlap population of V–O bond in R phase is about 0.556. The average overlap population in M1 phase is also calculated to be about 0.36. The absolute value of the bond population reflects the level of covalence properties of V–O bond in both phase, and also means the extent of the

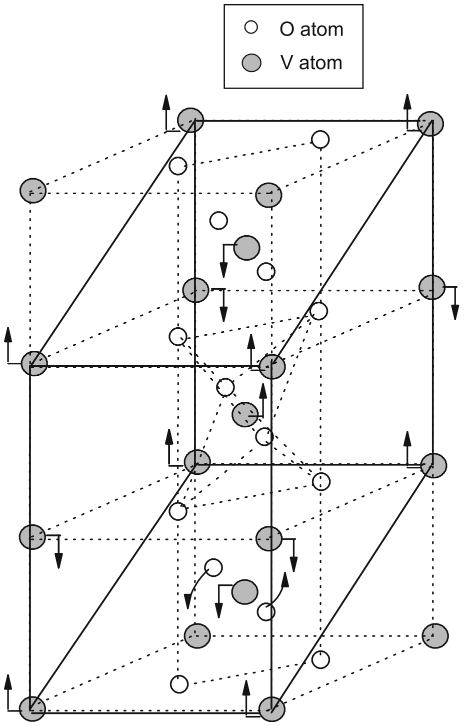

Fig. 1 Crystal structures of the high-temperature rutile (R) tetragonal cell (*dotted line*) and low-temperature M1 unit cell (*solid line*). The *arrows* indicate the distortions from R to M1 phase, and the displacements of O atoms are given only for two inequivalent O's

electron sharing between them. The ratio of the covalence level between R and M1 phases is about 1.5, independent of U_{eff}.

Then, we calculate the band structures with varying U_{eff} of R and M1 phases, respectively. The calculated energy gap (E_g) curves are plotted in Fig. 2 versus varying U_{eff}. From Fig. 2, the MIT processes have been observed both in R and M1 structures by increasing the on-site Coulomb repulsion interaction U_{eff}. So, our results show that the MIT in such system is independent of the structure phase transition. However, their critical Coulomb repulsion $U_{\mathrm{eff}}^{\mathrm{C}}$ are different: 2.8 eV for R phase and 3.98 eV for M1 phase. Furthermore, their transition characters are absolutely dissimilar. Unlike that in the R phase, the MIT in monoclinic phase takes place suddenly, and an energy gap ($E_g \sim 0.32$ eV) opens abruptly at the critical point $U_{\mathrm{eff}}^{\mathrm{C}} \sim 3.98$ eV. The energy band of monoclinic VO_2 at the critical point is shown in Fig. 3. It is obvious that the energy gap ($E_g \sim 0.32$ eV) is an indirect gap between two symmetry points B and D in Brillouin zone with different momentum. Nevertheless, the direct energy gap at the same symmetry point D is about 0.58 eV. The indirect energy gap ($\sim$0.32 eV) can be used to interpret the experimental 0.31 eV optical transmission observed by Verleur et al. [23] perfectly, but the authors had attributed it to the free-carrier-dominated behavior. The optical transition between two different symmetry points is usually electron phonon scattering required due to the momentum conservation, with low-excitation probability. As a result, the energy gap detected by optical experiment should usually be the direct energy gap. Therefore, our calculated direct energy gap ($\sim$0.58 eV) agrees to the experimental gap 0.6 eV given by Ladd and Paul from optical transmission experiment [45] very well. It is also consistent with the energy gap obtained by means of all-electron full-potential linear muffin-tin orbital GW calculation [14]. Unlike the transition in R structure, the sudden and sharp behavior at the phase transition in M1 structure is consistent with the experimental observation. We suggest that the MIT should take place in M1 phase with the first-order characters, although the MIT can occur in both R and M1 phases. And, the Hubbard U_{eff} of V atom in VO_2 should be around

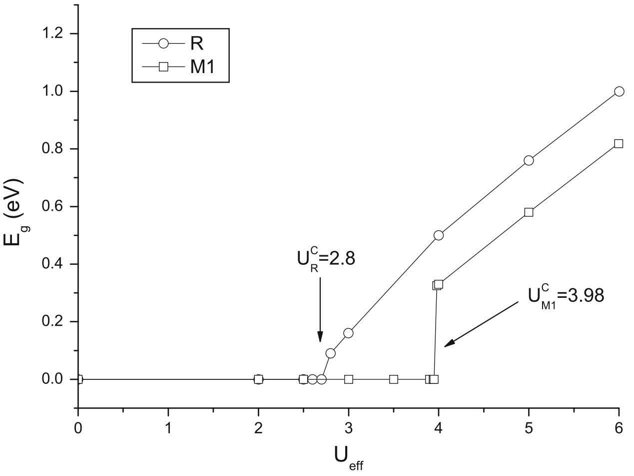

Fig. 2 The energy gap (E_g) curves of VO_2 with M1 and R phases versus varying U_{eff}

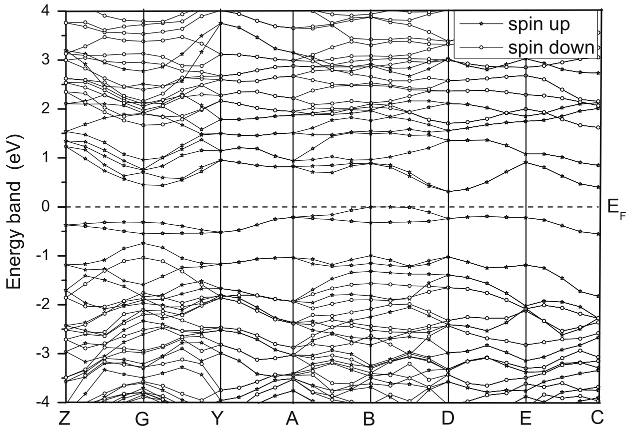

Fig. 3 The energy band structure of monoclinic VO_2 with M1 phase at $U_{\mathrm{eff}} = 3.98$

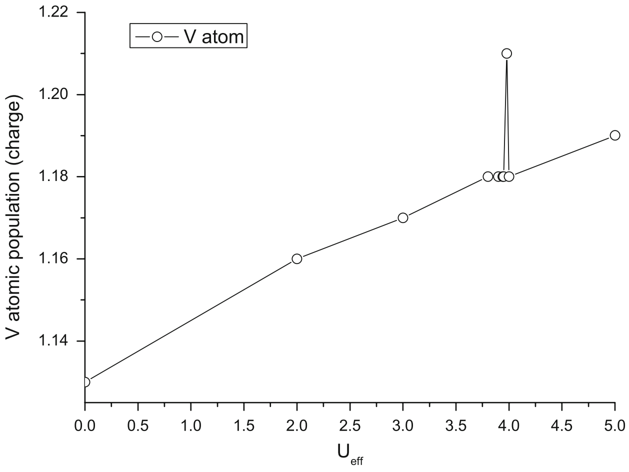

Fig. 4 The atomic population (charge) of V in monoclinic VO_2 with different U_{eff}

3.98 eV, which is nearly the same as that suggested in Ref. [13] on the basis of cluster dynamical mean-field theory.

In order to detect the charge transfer or electron occupation in M1 phase with the varying on-site correlation effects, we do some Mulliken analysis on the V atoms. The atomic population (charge) of V atoms is shown in Fig. 4. The positive charge of V ions increases slowly with enhanced correlation, but a distinct saltation of charge emerges at the critical point $U_{eff} = 3.98$ eV. A discontinuous and abrupt charge-transfer from the center V atom to the six O ligands was found during MIT process. The electronic system itself (the Coulomb interaction between electrons) can cause dramatic discontinuous MIT without any other effects (structural distortion or phonon). It means the correlation effects prevail upon the itinerancy of the electrons, forcing them to localize during the MIT process. Such character suggests the insulating M1 VO_2 a charge-transfer like insulator [46, 47].

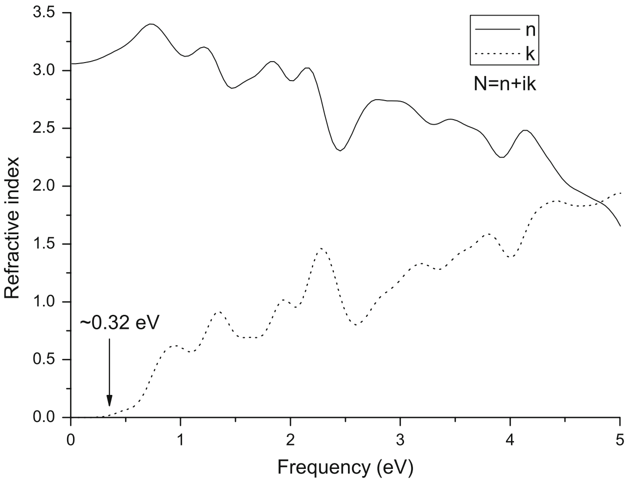

Fig. 5 The complex refractive index of monoclinic VO_2 with different U_{eff}

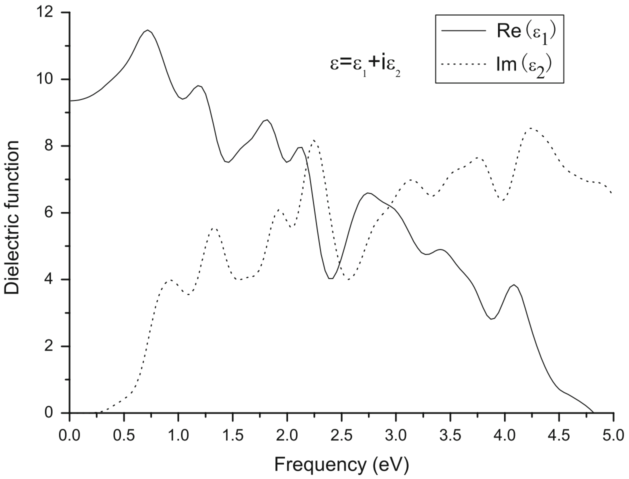

Fig. 6 The complex dielectric function of monoclinic VO_2

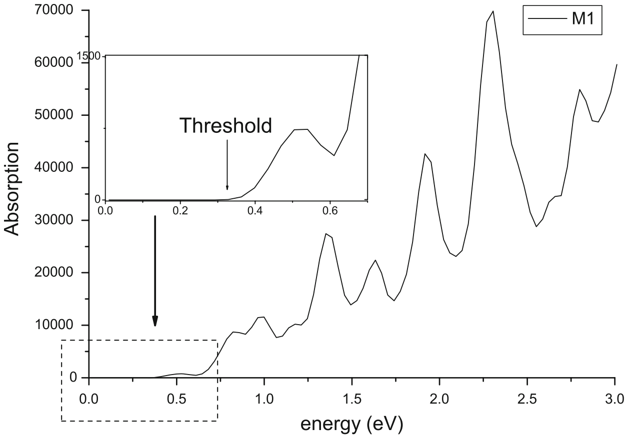

Fig. 7 The absorption spectrum of monoclinic VO_2

Finally, we calculate the optical constants of the M1 phase VO_2 at 300 K, including refractive index, dielectric constant, and absorption spectrum (as shown in Figs. 5, 6, and 7 respectively). The complex refractive index is plotted in Fig. 5. A distinct threshold at about 0.32 eV can be seen clearly in Fig. 5, below which the refractive index is absolutely real. We know that a real refractive index denotes the transparency of material, and such phenomena are consistent with the experimental optical transmission at 0.31 eV [23]. The real part ε_1 and imaginary part ε_2 of dielectric constant have also been obtained (as shown in Fig. 6). In Fig. 6, the imaginary part ε_2 of the dielectric constant shows two thresholds (at $\sim$0.3 and 0.6 eV) and several singularities at 0.88, 1.32, 1.9, 2.3, 2.7, and 3.6 eV. The two thresholds denote the optical transmission and the optical energy gap, respectively. And, these imaginary part singularities denote the corresponding optical absorption peaks. Furthermore, the absorption spectrum is plotted in Fig. 7. Except for a threshold at 0.31 eV and a little shoulder at about 0.6 eV, one can see some distinct absorption peaks set at 0.82, 0.99, 1.2, 1.34, 1.63, 1.93, 2.3, 2.6, 2.8, 3.1, 3.2, 3.4, and 3.6 eV, respectively. To sum up, all of the theoretical optical results above are consistent with each other, and they agree with the experimental absorption peaks(0.85, 1.04, 1.3(1.32), 1.82, 2.64, 2.8, and 3.6 eV) [23, 25] very well. Additionally, the threshold at 0.31 eV should be the optical transmission point, and the little shoulder around 0.6 eV should be the optical observation energy gap.

Conclusion

In the present article, we have made some Mulliken analysis of the V–O bond, first. The overlap population of them is found to depend on the bond length between O and V sensitively, but to be independent of the on-site Coulomb interaction on V atoms. The level of covalence of R phase are stronger than that of M1 phase, the ratio average overlap population between R and M1 phases is about 1.5.

Consequently, we have calculated the band structure and the energy gap of both high temperature R and low temperature M1 structure VO_2. Our calculations show that, though the MIT can take place in both structures by increasing the on-site Coulomb repulsion interaction, the sudden and abrupt opening of the energy gap of M1 phase is consistent with the experimental observations. The M1 VO_2 belongs to an indirect gap semiconductor with an indirect energy gap $\sim$0.32 eV, which interprets the experimental 0.31 eV optical transmission. Furthermore, the direct energy gap about 0.58 eV agrees to the experimental gap 0.6 eV very well. According to our calculation, we suggest that the MIT should take place in M1 phase without any structural changes, and have the first-order characters.

Then, we have investigated the charge transfer or electron occupation in M1 phase with varying correlated effects. The Mulliken analysis on the V atoms has been made. A discontinuous and abrupt charge-transfer from the center V atom to the six O ligands, and a strong electronic localization has been found during MIT process. Such character suggests that the M1 VO_2 should be a charge-transfer like insulator.

Finally, we have calculated the optical properties of the M1 phase VO_2. Two thresholds (at $\sim$0.3 and 0.6 eV) are observed in the complex refractive index, the dielectric constant, and the absorption spectrum. And, the threshold at 0.31 eV should be the optical transmission point, and the little shoulder around 0.6 eV should be the optical energy gap. The theoretical results agree with the experimental observation very well.

Acknowledgements This work is supported by the major research program from the Ministry of Science and Technology of China under Grant No. 2009CB939901. Numerical computation of this work was carried out on the Parallel Computer Cluster of Institute for Condensed Matter Physics (ICMP) at School of Physics, Peking University.

References

1. Morin J (1959) Phys Rev Lett 3:34
2. Takayuki U, Kozo O, Akio K (1993) J Phys Soc Jpn 62:2595
3. Goering E, Schramme M, Müller O, Barth R, Paulin H, Klemm M, Denboer ML, Horn S (1997) Phys Rev B 55:4225
4. Kim H-T, Chae B-G, Youn D-H, Maeng S-L, Kim G, Kang K-Y, Lim Y-S (2004) New J Phys 6:52
5. Kim H-T, Chae B-G, Youn D-H, Lee S-J, Kim K, Lim Y-S (2005) Appl Phys Lett 86:242101
6. Kim B-J, Lee YW, Choi S, Lim JW, Yun SJ, Kim H-T, Shin T-J, Yun H-S (2008) Phys Rev B 77:235401
7. Eguchi R, Taguchi M, Matsunami M, Horiba K, Yamamoto K, Ishida Y, Chainani A, Takata Y, Yabashi M (2008) Phys Rev B 78:075115
8. Xu SQ, Ma HP, Dai SX, Jiang ZG (2004) J Mater Sci 39:489. doi: 10.1023/B:JMSC.0000011503.22893.f4
9. Gopalakrishnan G, Ruzmetov D, Ramanathan S (2009) J Mater Sci 44:5345. doi:10.1007/s10853-009-3442-7
10. Goodenough JB (1960) Phys Rev 117:1442
11. Wentzcovitch RM, Schulz WW, Allen PB (1994) Phys Rev Lett 72:3389
12. Rice TM, Launois H, Pouget JP (1994) Phys Rev Lett 73:3042
13. Biermann S, Poteryaev A, Lichtenstein AI, Georges A (2005) Phys Rev Lett 94:026404
14. Sakuma R, Miyake T, Aryasetiawan F (2008) Phys Rev B 78:075106
15. Koethe TC, Hu Z, Haverkort MW, Schüßler-Langeheine C, Venturini F, Brookes NB, Tjernberg O, Reichelt W, Hsieh HH, Lin H-J, Chen CT, Tjeng LH (2006) Phys Rev Lett 97:116402
16. Kim HT (2002) . Physica C 341–348:259
17. Brinkman WF, Rice TM (1970) Phys Rev B 2:4302
18. Boyce JB, Bridges FG, Claeson T, Geballe TH, Li GG, Sleight AW (1991) Phys Rev B 44:6961
19. Arcangeletti E, Baldassarre L, Castro DDi, Lupi S, Malavasi L, Marini C, Perucchi A, Postorino P (2007) Phys Rev Lett 98:196406
20. Moore RG, Zhang J, Nascimento VB, Jin R, Guo Jiandong, Wang GT, Fang Z, Mandrus D, Plummer EW (2007) Science 318:615
21. Berglund CN, Guggenheim HJ (1969) Phys Rev 185:1022
22. Barker AS Jr, Verleur HW, Guggenheim HJ (1966) Phys Rev Lett 17:1286
23. Verleur HW, Barker AS Jr, Berglund CN (1968) Phys Rev 172:788
24. Paul W (1970) Mat Res Bull 5:691
25. Gavini A, Kwan CCY (1972) . Phys Rev B 5:3138
26. Cramer CJ, Truhlar DG (2009) Phys Chem Chem Phys 11:10757
27. Cohen AJ, Mori-Sánchez P, Yang W (2008) Phys Rev B 77:115123
28. Cohen AJ, Mori-Sánchez P, Yang W (2008) Science 321:792
29. Mosey NJ, Liao P, Carter EA (2008) J Chem Phys 129:014103
30. Mori-Sánchez P, Cohen AJ,Yang W (2009) Phys Rev Lett 102:066403
31. Janesko BG, Henderson TM, Scuseria GE (2009) Phys Chem Chem Phys 11:443
32. Nieminen RM (2009) Modelling Simul Mater Sci Eng 17:084001
33. Segall MD, Lindan PLD, Probert MJ, Pickard C, Hasnip PJ, Clark SJ, Payne MC (2002) J Phys Condens Matter 14:2717
34. Hammer B, Hansen LB, Norskov JK (1999) Phys Rev B 59:7413

35. Perdew JP, Wang Y (1992) Phys Rev B 45:13244
36. Vanderbilt D (1990) Phys Rev B 59:7892
37. Anisimov V, Zaanen J, Andersen OK (1991) Phys Rev B 44:943
38. Cococcioni M, De Gironcoli S (2005) Phys Rev B 71:035105
39. Dudarev SL, Botton GA, Savrasov SY, Humphreys CJ, Sutton AP (1998) Phys Rev B 57:1505
40. Mulliken RS (1955) J Chem Phys 23:1833
41. Davidson ER, Chakravorty S (1992) Theor Chim Acta 83:319
42. Segall MD, Pickard CJ, Shah R, Payne MC (1996) Phys Rev B 54:16317
43. McWhan DB, Marezio M, Remeika JP, Dernier PD (1974) Phys Rev B 10:490
44. Longo JM, Kierkegaard P (1970) Acta Chim Scand 24:420
45. Ladd LA, Paul W (1969) Solid State Commun 7:425
46. Chung W, Freericks JK (1998) Phys Rev B 57:11955
47. Hague CF, Mariot J-M, Ilakovac V, Delaunay R (2008) Phys Rev B 77:045132